Clinical Cancer Research

A Novel Murine GITR Ligand Fusion Protein Induces Antitumor Activity as a Monotherapy That Is Further Enhanced in Combination with an OX40 Agonist

Rebecca Leyland[1], Amanda Watkins[1], Kathy A. Mulgrew[2], Nicholas Holoweckyj[2], Lisa Bamber[1], Natalie J. Tigue[1], Emily Offer[1], John Andrews[1], Li Yan[3], Stefanie Mullins[1], Michael D. Oberst[2], Jane Coates Ulrichsen[1], David A. Leinster[1], Kelly McGlinchey[2], Lesley Young[1], Michelle Morrow[1], Scott A. Hammond[2], Philip Mallinder[1], Athula Herath[1], Ching Ching Leow[2], Robert W. Wilkinson[1], and Ross Stewart[1]

Abstract

Purpose: To generate and characterize a murine GITR ligand fusion protein (mGITRL-FP) designed to maximize valency and the potential to agonize the GITR receptor for cancer immunotherapy.

Experimental Design: The EC_{50} value of the mGITRL-FP was compared with an anti-GITR antibody in an *in vitro* agonistic cell–based reporter assay. We assessed the impact of dose, schedule, and Fc isotype on antitumor activity and T-cell modulation in the CT26 tumor model. The activity of the mGITRL-FP was compared with an agonistic murine OX40L-FP targeting OX40, in CT26 and B16F10-Luc2 tumor models. Combination of the mGITRL-FP with antibodies targeting PD-L1, PD-1, or CTLA-4 was analyzed in mice bearing CT26 tumors.

Results: The mGITRL-FP had an almost 50-fold higher EC_{50} value compared with an anti-murine GITR antibody. Treatment of CT26 tumor-bearing mice with mGITRL-FP–mediated significant antitumor activity that was dependent on isotype, dose, and duration of exposure. The antitumor activity could be correlated with the increased proliferation of peripheral $CD8^+$ and $CD4^+$ T cells and a significant decrease in the frequency of intratumoral Tregs. The combination of mGITRL-FP with mOX40L-FP or checkpoint inhibitor antagonists enhanced antitumor immunity above that of monotherapy treatment.

Conclusions: These results suggest that therapeutically targeting GITR represents a unique approach to cancer immunotherapy and suggests that a multimeric fusion protein may provide increased agonistic potential versus an antibody. In addition, these data provide, for the first time, early proof of concept for the potential combination of GITR targeting agents with OX40 agonists and PD-L1 antagonists. *Clin Cancer Res; 23(13); 3416–27. ©2017 AACR.*

Introduction

The function of T cells is tightly regulated to maintain peripheral tolerance and ensure their safe and effective activation. One critical mechanism of control is a series of cell surface receptors, expressed on T cells themselves, which deliver inhibitory or stimulatory cosignals in a spatially and temporally controlled manner to control T-cell activation in response to antigen. Complementing these signals are a range of specialized cell types, such as regulatory T cells (Tregs), that function to suppress or direct T-cell activation through a range of mechanisms (1).

Glucocorticoid-induced TNFR-related protein (GITR) is one of a number of TNFR superfamily members expressed on the surface of activated T cells; others include OX40, CD137, and CD27. The interaction between GITR and its ligand delivers positive costimulatory signals to T cells, which enhance their proliferation and activation (2, 3) and increase their resistance to suppression by Tregs (4–7). These signals have also been demonstrated to directly modulate the function and reduce the stability of Tregs (8–10).

Targeting murine GITR with the agonistic antibody DTA-1 has demonstrated significant antitumor activity in a range of murine models of cancer (4, 11–14). In at least one study (15), this antitumor activity was enhanced through the use of a murine IgG2a (mIgG2a) antibody that strongly engaged Fc gamma receptors (FcγR) and led to depletion of intratumoral Tregs, but was completely abrogated through the introduction of mutations that eliminated all FcγR binding.

The binding of GITR ligand (GITRL) to GITR results in multimerization of the GITR receptor. This, in turn, allows for recruitment of downstream signaling adaptors called TNFR-associated factors (TRAF) that mediate the activation of downstream signaling pathways such as nuclear factor kappa B (NFκB) and mitogen-activated protein kinase (MAPK) (16). Higher order structures of GITRL are believed to mediate stronger signals through their ability to drive greater aggregation of GITR (17, 18). The requirement for

[1]MedImmune Ltd., Granta Park, Cambridge, United Kingdom. [2]MedImmune LLC, One MedImmune Way, Gaithersburg, Maryland. [3]MedImmune LLC, Mountain View, California.

Note: Supplementary data for this article are available at Clinical Cancer Research Online (http://clincancerres.aacrjournals.org/).

Corresponding Author: Robert Wilkinson, MedImmune Ltd., Aaron Klug Building, Granta Park, Cambridge, CB21 6GH, United Kingdom. Phone: 44 (0) 203 749 6665; Fax: 44 (0) 1223 471472; E-mail: wilkinsonr@medimmune.com

doi: 10.1158/1078-0432.CCR-16-2000

Translational Relevance

Several GITR-targeting agents are already in clinical trials for the treatment of cancer. Here we describe the preclinical characterization of a mouse GITR ligand fusion protein (mGITRL-FP) designed to maximize valency and the potential to agonize the GITR receptor. We expand on the role of Fc isotype requirement for GITR-targeting agents, identify pharmacodynamic biomarkers of activity, and explore how dosing influences antitumor activity and T-cell proliferation. We also investigate the mechanisms of combining the mGITRL-FP with an OX40 agonist or checkpoint inhibitor antagonists. The data in this manuscript provide evidence that therapeutic targeting of GITR represents a unique approach to cancer immunotherapy, distinct and nonredundant to OX40 targeting, and suggest that a multimeric fusion protein may provide increased agonistic potential versus an antibody. Importantly, this report is the first to show a beneficial effect from targeting the GITR pathway in combination with an OX40 agonist or PD-L1 antagonist.

FcγR binding observed for the antitumor activity of DTA-1 may be explained by the need for higher order clustering to mediate effective signaling through GITR, and is a phenomenon that has also been observed for antibodies directed against other TNFR superfamily proteins (19), including OX40 (20).

Here we describe the generation and characterization of a mouse GITRL fusion protein (mGITRL-FP) designed to maximize valency and the potential to agonize the GITR receptor. We demonstrate the ability of this mGITRL-FP to drive significant antitumor activity, and dissect the mechanism of action using molecules with different Fc isotypes, which have differential abilities to agonize or deplete GITR-expressing cells. Furthermore, through pharmacodynamic (PD) and combination studies with a murine OX40 ligand (OX40L) FP, we show nonredundant and unique roles for GITR and OX40 agonism with respect to stimulating antitumor immunity. Finally, we establish proof of concept for mGITRL-FP as a robust combination partner for molecules targeting checkpoint inhibitors.

Materials and Methods

Cell line generation

Jurkat mGITR NFκB cell line was generated in house by lentiviral transduction using a third-generation lentiviral system (Systems Biosciences). The murine Gitr gene (NM_009400.2) was cloned into the expression plasmid under the control of a CAG promoter and containing a puromycin-resistant gene. The NFκB reporter expression plasmid was designed to express five copies of the NFκB response element under a minimal promoter and upstream of a firefly luciferase reporter (luc2; Promega), together with a blasticidin-resistant gene. Each expression plasmid alongside the packaging plasmids (Systems Biosciences) were cotransfected into HEK293T-17 using Lipofectamine 2000 (Invitrogen). Supernatant containing viral particles was collected 48 hours post-transfection and used to transduce Jurkat cells. Virally transduced Jurkat cells were cultured in culture media plus selection antibiotics, 5 μg/mL blasticidin, and 5 μg/mL puromycin from 48 hours post-transduction. Jurkat human OX40 NFκB cell line was generated using similar procedures, except a lentiviral vector designed to constitutively express human OX40 was transduced. Mouse OX40L binds to human OX40; therefore, a human OX40-expressing NFκB luciferase reporter Jurkat cell line can be used to assess the activity of murine OX40L fusion proteins.

NFκB reporter assay

Jurkat mGITR or human OX40 NFκB cells were cultured at 37°C, 5% CO_2, and 85% humidity in 96-well plates at 5×10^4 cells (Jurkat mGITR) or 2×10^5 cells (Jurkat human OX40)/well together with anti-GITR antibody DTA-1 (Biolegend), NIP rIgG2b isotype control (made in-house), mGITRL-FP mIgG2a or plate immobilized mOX40L-FP mIgG1 or isotype control [comprised a single amino acid mutation at a position (Y182A) that rendered the protein unable to signal via OX40] as indicated. Steady Glo Reagent (Promega) containing luciferin substrate was added to the plates after 5 hours or after 16 hours for assays containing mOX40L-FP mIgG1 and the plates were incubated for 30 minutes in the dark on a plate shaker. Assay signal was detected using an Envision plate reader (Perkin Elmer).

SDS-PAGE

Five micrograms of protein was mixed with loading buffer and reducing agent, denatured at 80°C for 10 minutes and loaded onto a 4%–20% Tris-Glycine SDS-PAGE gel (Thermo Fisher Scientific), alongside a protein molecular weight marker (Rainbow Marker, GE Healthcare). The proteins were electrophoresed for 45 minutes at 200 V and stained using Instant Blue protein stain (Sigma).

Mice and tumor models

Eight- to 10-week-old BALB/c or C57BL/6 female mice were obtained from Charles River UK Ltd. or Harlan Laboratories Inc. For studies performed in the United States, mice were housed in an Association for Assessment and Accreditation of Laboratory Animal Care (AAALAC)-accredited and United States Department of Agriculture (USDA)-licensed facility under sterile and standardized environmental conditions. For studies performed in the United Kingdom, experiments were conducted under a United Kingdom. Home Office Project License in accordance with the U. K. Animal (Scientific Procedures) Act 1986 and in accordance with EU Directive EU 2010/63. A 100-μL suspension of CT26 (ATCC) or B16F10-Luc2 cells in PBS at a cell density of 5×10^6 cells/mL or 5×10^4 cells/mL were subcutaneously injected into the right flank of each animal. The B16F10-Luc2 cell line was generated through lentiviral transduction of the B16F10 cell line (ATCC) with a construct expressing a luciferase reporter under the control of the CAG promoter and was implanted in 50% PBS and 50% growth factor–reduced and phenol red–free Matrigel (Corning). Cell lines were cultured to limited passage before implantation and were periodically screened to confirm the absence of mycoplasma. Cells were further authenticated via STR profiling (IDEXX Bioresearch) and screened for a panel of mouse viruses (Charles River). Measurable tumors were randomized on the basis of tumor volume into respective groups. The length (mm) and width (mm) of each tumor was measured with an electronic caliper 3 times per week. Volumes of tumors (mm^3) were calculated on the basis of the formula [length (mm) × width $(mm)^2$]/2. Tumor growth responses were categorized as a response if there was no measureable tumor or a sustained tumor growth inhibition such

that volume was less than 200 mm^3 at the end of the study. Number of regressions indicated on each spider plot is relative to the total number of tumors implanted. Power calculation was performed to determine group sizes for *in vivo* studies. Mice were dosed intraperitoneally with either mGITRL-FP, mOX40L-FP, NIP228 mIgG1 D265A, anti-programmed death ligand 1 (PD-L1) mIgG1 D265A, anti-cytotoxic T-lymphocyte associated antigen-4 (CTLA-4) mIgG2b (clone 9D9, BioXcell), or anti-programmed cell death protein-1 rIgG2a (PD-1, clone RMP1-14, BioXCell). NIP228 and PD-L1 were engineered in-house to have an amino acid substitution of aspartate to alanine at position 265 to limit the binding to FcγRs (21). Mice were dosed at the indicated time points as written in the text or when the tumors reached a volume of 200 mm^3. Dosing of 25 mg/kg mGITRL-FP in B16F10-Luc2–bearing mice was only tolerated for four doses.

Flow cytometry

Tumor, spleen, or tumor draining lymph node were dissected and placed into RPMI1640 media on ice. Tissues were disaggregated by passing each through a 40- or 100-μm nylon cell strainer (Falcon), and cells were pelleted by centrifugation and resuspended in red blood cell lysis buffer (Sigma). Following incubation for 2 minutes at room temperature, cells were washed and resuspended in flow cytometry buffer (eBioscience). Tumor tissue samples were processed using the gentle MACS Dissociator and Tumor Dissociation Kit (Miltenyi Biotec) following manufacturer's instructions.

Samples were stained for viability using live dead fixable blue (Life Technologies) following manufacturer's instructions and then blocked with anti-CD16/32 (eBioscience) before staining with fluorochrome-conjugated antibodies. CD4 (Rm4.5), Foxp3 (FJK-16S), Ki67 (Sol A15), ICOS (7E.17G9), Eomes (Dan11mag), T-bet (Apr-46), and GITR (DTA-1) were purchased from eBioscience. CD45 (30-F11), CD44 (IM7), CD62L (MEL-14), PD-1 (29F.1A12), and OX40 (OX86) were purchased from Biolegend. CD8 (53–6.7) was purchased from BD Pharmingen. For staining of intracellular antigens, the Foxp3 Staining Kit (eBioscience) was used according to manufacturer's instructions. Samples were fixed in 3.7% formalin before acquisition of samples using a Fortessa (Becton Dickinson). Data were analyzed with FlowJo software.

Pharmacokinetic modeling

Balb/c mice were administered 5 or 15 mg/kg mGITRL-FP mIgG2a once. Three mice per group were sacrificed 5 minutes, 0.5, 1, 2, 6, 24, 72, 144, and 240 hours following treatment. Serum samples were collected and the levels of circulating mGITRL-FP mIgG2a present were assessed in a sandwich ELISA using anti-murine GITRL mAb (R&D Systems) as both capture and detection.

Pharmacokinetic data obtained from the two dosing groups were pooled and simultaneously modeled using a nonlinear mixed effects modeling approach with the software package NONMEM (Version 7.2, ICON Development Solutions). The first-order conditional estimation (FOCE) with Interaction method was used. Murine GITRL-FP mIgG2a pharmacokinetics was adequately descripted by a two-compartment model.

Statistical analysis

All statistical analysis was carried out using the Prism Statistical Software Version 6.

Results

A murine GITR ligand fusion protein has enhanced *in vitro* potency compared with the anti-murine GITR antibody, DTA-1

To investigate the effects of GITR receptor signaling on immune cell activation and antitumor activity *in vivo*, a tetrameric mGITRL-FP was generated. The mGITRL-FP was designed to elicit avid binding to the GITR receptor and FcγRs on effector cells. The molecule consisted, from N- to C-terminus, of a fragment crystallizable (Fc) region of an immunoglobulin G (IgG), the yeast-derived coiled coil GCN4 pII and the extracellular (GITR-binding) domain (ECD) of murine GITR ligand (Fig. 1A; Supplementary Fig. S1). When the purified denatured mGITRL-FP was visualized by SDS-PAGE (Fig. 1B), it demonstrated a high degree of homogeneity and a molecular weight that was slightly higher than the expected molecular weight of 48 kDa presumably due to glycosylation of the Fc and mGITRL domains. Both mGITRL-FP mIgG2a and an anti-GITR antibody (DTA-1) were able to induce NFκB signaling in a GITR-dependent NFκB reporter gene cell assay, whereas a murine OX40L-FP mIgG1 (mOX40L-FP mIgG1) and isotype control lacked any detectable signal (Fig. 1C). Importantly, the tetrameric mGITRL-FP demonstrated an EC_{50} of 0.05 nmol/L with respect to GITR agonism in this assay, which was nearly 50 times more potent than DTA-1, which demonstrated an EC_{50} of 2.31 nmol/L.

Comprehensive FcγR engagement increases antitumor activity but does not drive increased T-cell proliferation downstream of GITR

It has been reported previously that activating FcγRs are required for the antitumor activity of the DTA-1 antibody, and that the antitumor activity of this antibody is increased when it carries a mIgG2a Fc, compared with a rIgG2b Fc or a N297A mutant Fc which lacks FcγR binding (15). To determine the impact of the Fc isotype on the antitumor activity of mGITRL-FP, CT26 tumor–bearing mice were treated with mGITRL-FP with a mIgG2a or mIgG1 Fc isotype. Treatment of mice with 5 or 10 mg/kg of either isotype resulted in notable antitumor activity compared with saline-treated controls, as evidenced by reduced tumor volume (Fig. 2A). The antitumor activity overall, however, was greater following treatment with mGITRL-FP mIgG2a (13/20 total regressions), as opposed to mGITRL-FP mIgG1 (7/20 total regressions; Fig. 2A).

To determine whether this difference in activity of the Fc variants was due to a difference in their ability to mediate T-cell activation and subsequent events downstream of GITR agonism, the proliferation of splenic T-cell populations was assessed using flow cytometric analysis of Ki67 expression on $CD4^+$ $FoxP3^-$ (effector T cells), $CD8^+$ (effector T cells), and $CD4^+$ $FoxP3^+$ (Tregs) cells. Both isotypes of the mGITRL-FP caused a comparable significant increase in the proliferation of all three splenic T-cell subsets when compared with saline controls (Fig. 2B). The splenic Treg cell population exhibited the highest expression of Ki67 after treatment (53.95% ± 0.75% after mGITRL-FP mIgG2a and 58.43% ± 1.26% after mGITRL-FP mIgG1 treatment), followed by $CD4^+$ $FoxP3^-$ (9.52% ± 0.58% with mGITRL-FP mIgG2a and 10.89% ± 0.56% with mGITRL-FP mIgG1) and $CD8^+$ T cells (7.60% ± 0.27% with mGITRL-FP mIgG2a and 7.79 ± 0.43 with mGITRL-FP mIgG1). This data suggested that splenic T-cell activation alone could not account for the differences

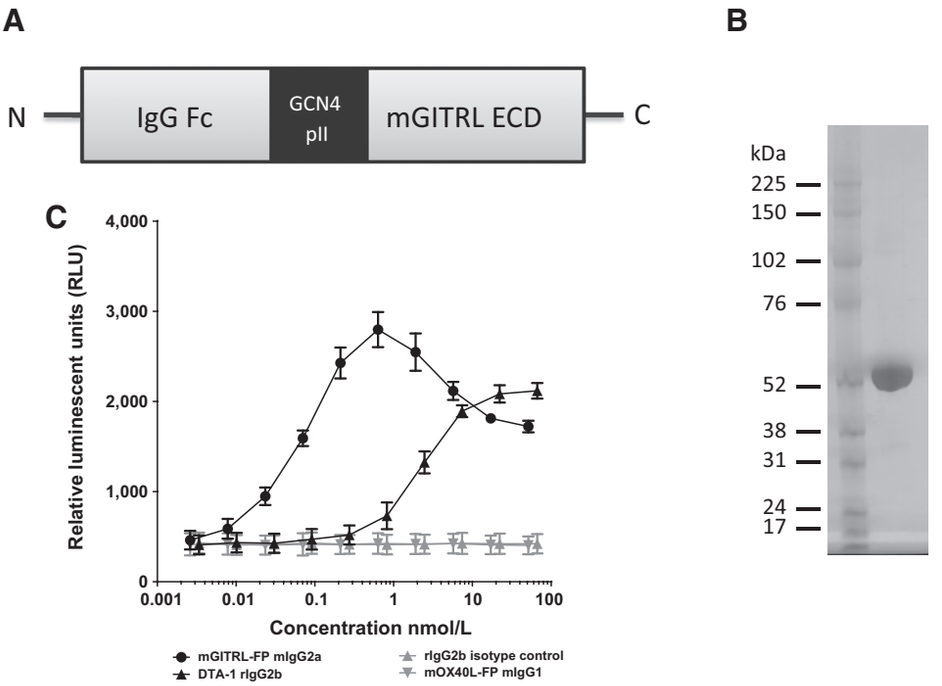

Figure 1.
Structure and agonistic potential of a murine GITR ligand fusion protein. **A,** Schematic of murine GITRL-FP consisting from N- to C-terminus, of a fragment crystallisable (Fc) region of an immunoglobulin G1 (IgG1) or 2a (IgG2a), a multimerization domain and the extracellular (GITR-binding) domain (ECD) of murine GITR ligand. **B,** SDS-PAGE of the purified murine GITRL-FP. **C,** NFκB-associated luminescence in a murine GITR receptor–transduced Jurkat cell line following treatment with mGITRL-FP, DTA-1, rIgG2b isotype controls, or mOX40L-FP. Data are representative of two independent experiments.

observed in antitumor immunity between mIgG1 and mIgG2a Fc isotypes of the mGITRL-FP.

We next investigated whether intratumoral changes in T-cell populations could explain the increased antitumor activity observed with the mIgG2a versus mIgG1 variants of mGITRL-FP. Treatment of mice with mGITRL-FP mIgG2a induced a significant decrease in the frequency of intratumoral Tregs from 13.31% ± 1.06% in saline-treated animals to 3.60% ± 0.79% with a significance value of $P < 0.0001$ (Fig. 2C; Supplementary Fig. S2) and a subsequent increase in the CD8:Treg (Fig. 2D) and CD4:Treg (Fig. 2E) ratios compared with saline-treated animals. In contrast, the decrease in intratumoral Tregs was not evident for the mIgG1 Fc variant of mGITRL-FP (12.95% ± 1.34%). There was also evidence for a significant decrease in the proportion of intratumoral $CD4^+$ $Foxp3^-$ T cells after treatment with mGITRL-FP mIgG2a (8.64% ± 1.21%) compared with control animals (13.01% ± 1.12%), but this was not to the extent of that observed for Tregs. The preferential depletion of Tregs by mGITRL-FP mIgG2a is likely attributable to the high expression of GITR on intratumoral Tregs (Fig. 2F) and the high expression of activating FcγRs in the tumor microenvironment of CT26 tumors (15), and is suggestive of clearance by antibody-dependent cellular cytotoxicity (ADCC) or antibody-dependent cellular phagocytosis (ADCP). Collectively, these data suggest that for optimal antitumor activity following mGITRL-FP treatment, proliferation of peripheral $CD4^+$ and $CD8^+$ T cells coincident with a decrease in intratumoral Tregs is required.

Murine GITRL-FP mIgG2a mediates antitumor activity and pharmacodynamic biomarker changes in a dose- and schedule-dependent manner

Because mGITRL-FP mIgG2a elicited increased antitumor activity compared with the mGITRL-FP mIgG1, we next characterized how exposure levels and time of exposure of the mGITRL-FP mIgG2a in the blood related to antitumor responses in CT26 tumor-bearing mice. We first measured the effect of increasing dose level on tumor growth by treating mice with one single dose of saline control or 0.2, 1, or 5 mg/kg mGITRL-FP mIgG2a. Treatment with 0.2 mg/kg mGITRL-FP mIgG2a resulted in only 1 of 10 complete regressions; however, there was evidence for a dose-dependent increase in antitumor immunity when the dose was raised from 0.2 to 1 mg/kg or 5 mg/kg, which resulted in 6/10 and 9/10 regressions, respectively (Fig. 3A). Furthermore, the antitumor activity could also be improved by increasing the frequency of 0.2 mg/kg dosing to once every day or once every week (Fig. 3B). These results indicated that there was a required exposure level of mGITRL-FP mIgG2a needed to induce optimal antitumor activity, as defined by complete tumor regression or minimal residual tumor volume, which was reached only when using the once daily schedule. To determine this threshold, a pharmacokinetic model was developed using the mouse blood concentration data from two alternative dose levels of mGITRL-FP mIgG2a (5 and 15 mg/kg). This pharmacokinetic model was subsequently used to simulate the steady-state concentration of mGITRL-FP mIgG2a in mice receiving 0.2 mg/kg mGITRL-FP mIgG2a once daily or once every week, respectively (Fig. 3C). From the simulation, a threshold concentration of 1 μg/mL was considered relevant to optimal antitumor activity in mice.

We next sought to define pharmacodynamic biomarkers of activity, following mGITRL-FP mIgG2a treatment. The expression of Ki67 was used to assess proliferation, whereas ICOS, PD-1, and OX40, which are all known to be expressed on T cells following activation, were also analyzed. Increasing the exposure of mGITRL-FP mIgG2a, either by increasing the dose level or by increasing the frequency of administration, resulted in progressively greater increases in the frequency of Ki67, ICOS-, PD-1-, and OX40-expressing peripheral $CD4^+$ T cells

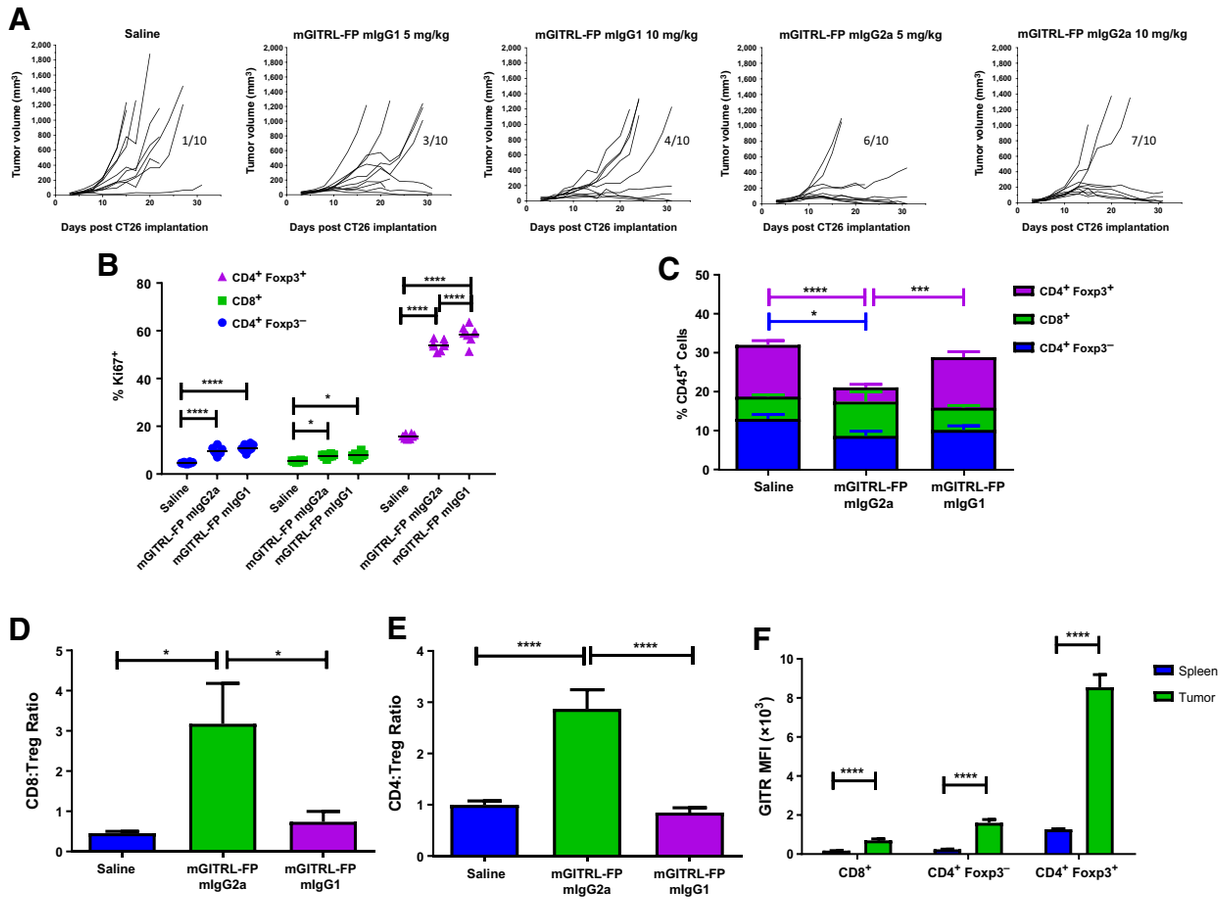

Figure 2.

Comprehensive FcγR engagement increases antitumor activity but does not drive increased T-cell proliferation downstream of GITR. **A,** Tumor growth in Balb/c mice. Mice were treated once by intraperitoneal injection of saline control, mGITRL-FP mIgG1, or mGITRL-FP mIgG2a as indicated. Number of regressions are indicated on each individual graph. **B,** Frequency of Ki67 expression in splenic T cells 4 days following treatment of CT26 tumor-bearing mice with 10 mg/kg mGITRL-FP or saline control. **C,** Frequency of intratumoral T-cell subsets. **D,** Ratio of intratumoral $CD8^+$ to $CD4^+$ $FoxP3^+$ cells or (**E**) ratio of intratumoral $CD4^+$ $Foxp3^-$ cells to $CD4^+$ $FoxP3^+$ cells 4 days following treatment of CT26 tumor-bearing mice with 10 mg/kg of mGITRL-FP or saline control as indicated. **F,** Median fluorescence intensity (MFI) of GITR expression on splenic and intratumoral T-cell subsets 10 days after CT26 implantation. Error bars, SEM; $n = 6$–10 mice per group. At least two independent experiments were carried out. **B** and **C,** *, $P < 0.05$; **, $P < 0.005$; ***, $P < 0.001$; and ****, $P < 0.0001$, as calculated by two-way ANOVA. Annotated significance for C is purple for changes in $CD4^+$ $Foxp3^+$cells and blue for changes in $CD4^+$ $Foxp3^-$ cells; **D** and **E**, *, $P < 0.05$; ****, $P < 0.0001$ as calculated by one way ANOVA; **F**, ****, $P < 0.0001$, as calculated by Student *t* test.

(Fig. 3D–G). Increases in the frequency of Ki67, ICOS, and PD-1 expressing peripheral $CD8^+$ T cells were also observed after treatment with mGITRL-FP mIgG2a compared with saline controls (data not shown).

Comparative analysis of mGITRL-FP and mOX40L-FP antitumor activity

The function and expression of GITR show some similarities to those of the TNFR family member OX40, a target for which a number of molecules are currently being tested clinically (22). To understand the mechanism of targeting GITR, as opposed to OX40, we directly compared the antitumor activities of the mGITRL-FP with a multimeric mOX40L-FP, which comprises a similar protein structure, does not cross react with the GITR receptor and is able to induce NFκB expression in an OX40 reporter cell assay (Supplementary Fig. S3A and S3B).

CT26 tumor-bearing mice were treated twice a week with 5 mg/kg mGITRL-FP or mOX40L-FP of either mIgG1 or mIgG2a Fc isotypes and tumor growth was measured. As seen with mGITRL-FP, the antitumor activity observed with mOX40L-FP was greater following treatment with the mIgG2a isotype (9/10 regressions) than with the mIgG1 (1/10 regressions; Fig. 4A). However, treatment with the mGITRL-FP mIgG1 (6/10 regressions) elicited increased antitumor activity relative to that seen following treatment with mOX40L-FP mIgG1 and was marginally better with a mIgG2a isotype (10/10) compared with mOX40L-FP mIgG2a (Fig. 4A). A similar depletion in intratumoral Tregs was observed following treatment with both mGITRL-FP and mOX40L-FPs with mIgG2a Fc isotypes, but this was not evident for mIgG1 Fc isotypes of either molecule (Fig. 4B). These data indicate that the mIgG2a isotype is superior to the mIgG1 for inducing antitumor activity of both GITR and OX40 agonists in CT26 tumor-bearing mice.

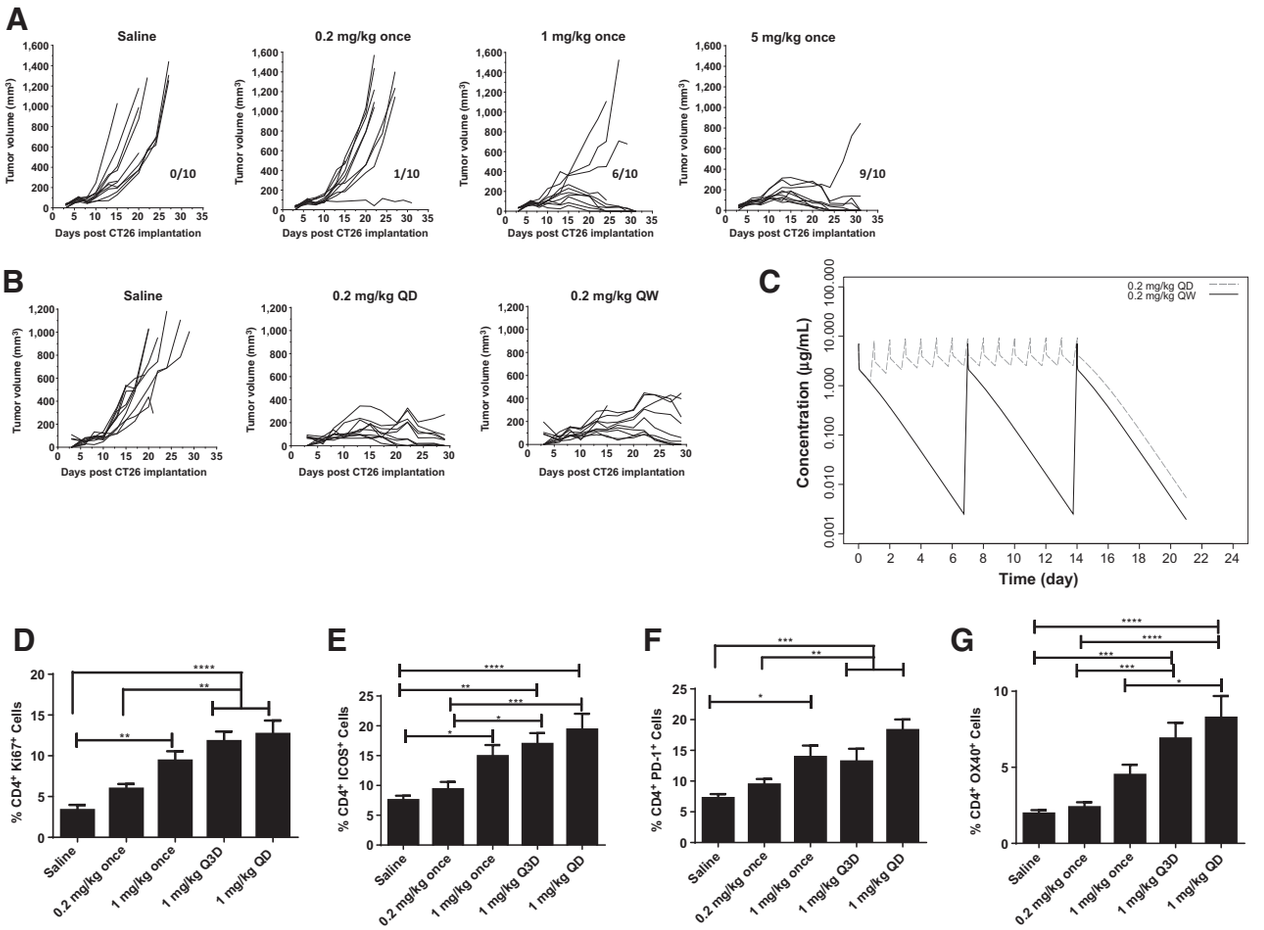

Figure 3.

Murine GITRL-FP mIgG2a mediates antitumor activity in a dose- and schedule-dependent manner. Tumor growth in Balb/c mice. Mice were treated by intraperitoneal injection of (**A**) a single dose of mGITRL-FP mIgG2a, at the dose level indicated or (**B**) multiple doses of 0.2 mg/kg mGITRL-FP mIgG2a given daily (QD) or weekly (QW). Data are one representative from at least two independent experiments. **C,** Predicted serum concentration of mGITRL-FP following administration using the dose and schedule indicated. Frequency of (**D**) Ki67, (**E**) ICOS, (**F**) PD-1, and (**G**) OX40-positive $CD4^+$ T cells in the tumor draining lymph node of CT26 tumor-bearing mice 7 days following treatment with 0.2 or 1 mg/kg mIgG2a mGITRL-FP once, every 3 days (Q3D) or every day (QD). Error bars represent the SEM from 7–8 mice per group. *, $P < 0.05$; **, $P < 0.01$; ***, $P < 0.001$; ****, $P < 0.0001$, as calculated by one-way ANOVA.

Combination of mGITRL-FP mIgG2a and mOX40L-FP mIgG1 leads to enhanced T-cell activation and antitumor activity

Given the upregulation of OX40 receptor on $CD4^+$ T cells following treatment with mGITRL-FP mIgG2a (Fig. 3G), we were interested to further dissect the potential to maximize T-cell activation. The mGITRL-FP mIgG2a and the mOX40L-FP mIgG1 were used to assess the potential benefits of combining agents targeting the GITR and OX40 pathways. These two molecules were chosen to maximize the translational relevance of these studies, because, despite their isotype mismatch, they represent the closest murine analogues for human GITRL (MEDI1873) and OX40L (MEDI6383) FPs currently in phase I clinical studies.

Biweekly treatment with mGITRL-FP mIgG2a and mOX40L-FP mIgG1 combination resulted in significantly increased expression of Ki67 in splenic $CD4^+$ (29.16% ± 1.51%) and $CD8^+$ (24.4% ± 0.87%) T cells compared with saline controls (7.82% ± 0.30% and 9.22% ± 0.31%) or treatment with either monotherapy (14.2% ± 0.45% and 15.52% ± 0.66% for mGITRL-FP–treated $CD4^+$ and $CD8^+$ T cells and 17.02% ± 0.49% and 16.22% ± 1.22% for mOX40L-FP–treated $CD4^+$ and $CD8^+$ T cells), showing an additive effect of combining both molecules (Fig. 5A). Additional analysis of the splenic $CD4^+$ and $CD8^+$ T-cell populations showed that combination treatment increased the frequency of both the $CD4^+$ and $CD8^+$ effector memory compartment, defined as $CD44^+$ and $CD62L^{lo}$ (Fig. 5B) and the $CD4^+$ central memory population, defined as $CD44^+$ and $CD62L^+$ (Fig. 5C) above that of monotherapy treatment. The expression of the transcription factors T-bet (Fig. 5D) and Eomes (Fig. 5E), which have shown redundancy in IFNγ production and cytotoxicity in $CD8^+$ T cells (23) and also have roles in Th1 differentiation, were also increased to a greater degree on $CD4^+$ and $CD8^+$ T cells during combination than with either monotherapy. A mechanistic difference between the GITR and OX40 pathways was the significantly higher expression of T-bet and Eomes on $CD4^+$

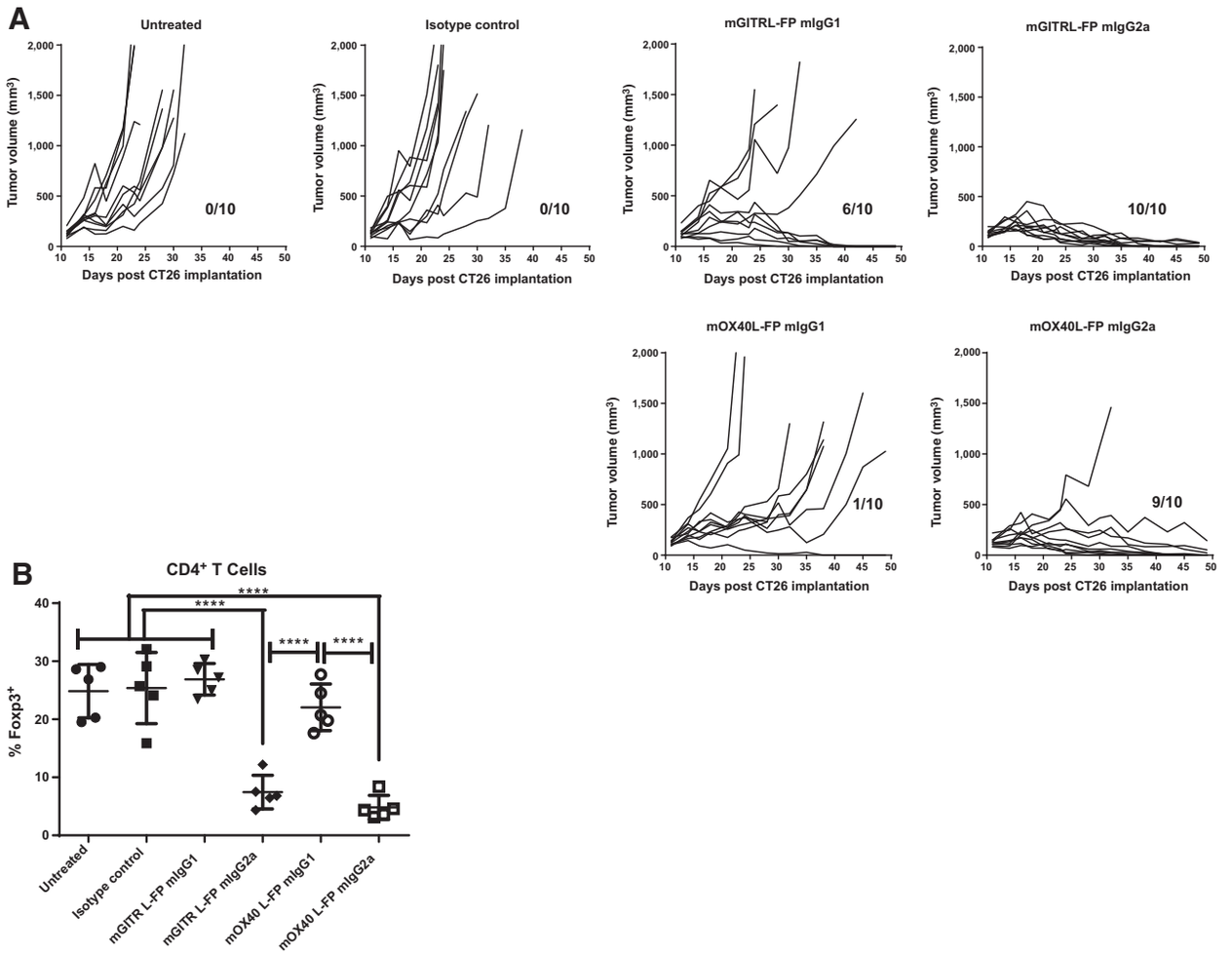

Figure 4.

Comparative analysis of mGITRL-FP and mOX40L-FP antitumor activity. **A,** Tumor growth in Balb/c mice. Mice were treated twice weekly with an intraperitoneal injection of 5 mg/kg mIgG2a or mIgG1 mGITRL-FP or mOX40L-FP, 5 mg/kg mIgG1 fusion protein isotype control or saline. Number of total regressions are indicated on each individual graph. **B,** Frequency of intratumoral $CD4^+$ $FoxP3^+$ Tregs in CT26 tumor-bearing Balb/c mice at 10 days following treatment as indicated. $N = 5$ mice per group. Error bars, SEM. *, $P < 0.05$; **, $P < 0.01$; ***, $P < 0.001$; ****, $P < 0.0001$, as calculated by one-way ANOVA. Data are one representative from at least two independent experiments.

T cells in mOX40L-FP mIgG1-treated animals as compared with animals treated with mGITRL-FP mIgG2a.

On the basis of these findings, we next determined the effect of combining mGITRL-FP mIgG2a with mOX40L-FP mIgG1 on tumor growth in this model. We investigated whether treatment of mice with mOX40L-FP mIgG1 could be further improved by combination with a single suboptimal dose of mGITRL-FP mIgG2a. Treatment with a suboptimal dose of mGITRL-FP mIgG2a monotherapy treatment induced 3/10 regressions, mOX40L-FP mIgG1 monotherapy induced 5/10 regressions, but the combination of both mGITRL-FP mIgG2a and mOX40L-FP mIgG1 resulted in enhanced antitumor activity showing 8/10 regressions (Fig. 5F).

Given that monotherapy treatment with mGITRL-FP mIgG2a at high doses induced complete tumor regression in the majority of mice in the CT26 model, we next asked whether the combination of high doses of mOX40L-FP mIgG1 and mGITRL-FP mIgG2a could offer increased benefit in a B16F10-Luc 2 model. Dosing with either monotherapy did not induce any tumor regression in this model; however, the combination of both molecules resulted in improved antitumor activity; a delay in tumor growth and increased survival compared with monotherapy treatment (Fig. 5G; Supplementary Fig. S4).

The mGITRL-FP synergizes with checkpoint inhibitors to induce antitumor activity in CT26 tumor-bearing mice

In addition to combining mGITRL-FP with mOX40L-FP, we also evaluated the potential to combine mGITRL-FP mIgG2a with antibodies targeting checkpoint inhibitors in the CT26 tumor model. Because PD-1 expression was shown to increase on $CD4^+$ T cells after treatment with mGITRL-FP mIgG2a (Fig. 3F), we next analyzed peripheral and intratumoral immune cells for expression of its partner PD-L1, in treated mice. Treatment with mGITRL-FP mIgG2a resulted in a significant upregulation of

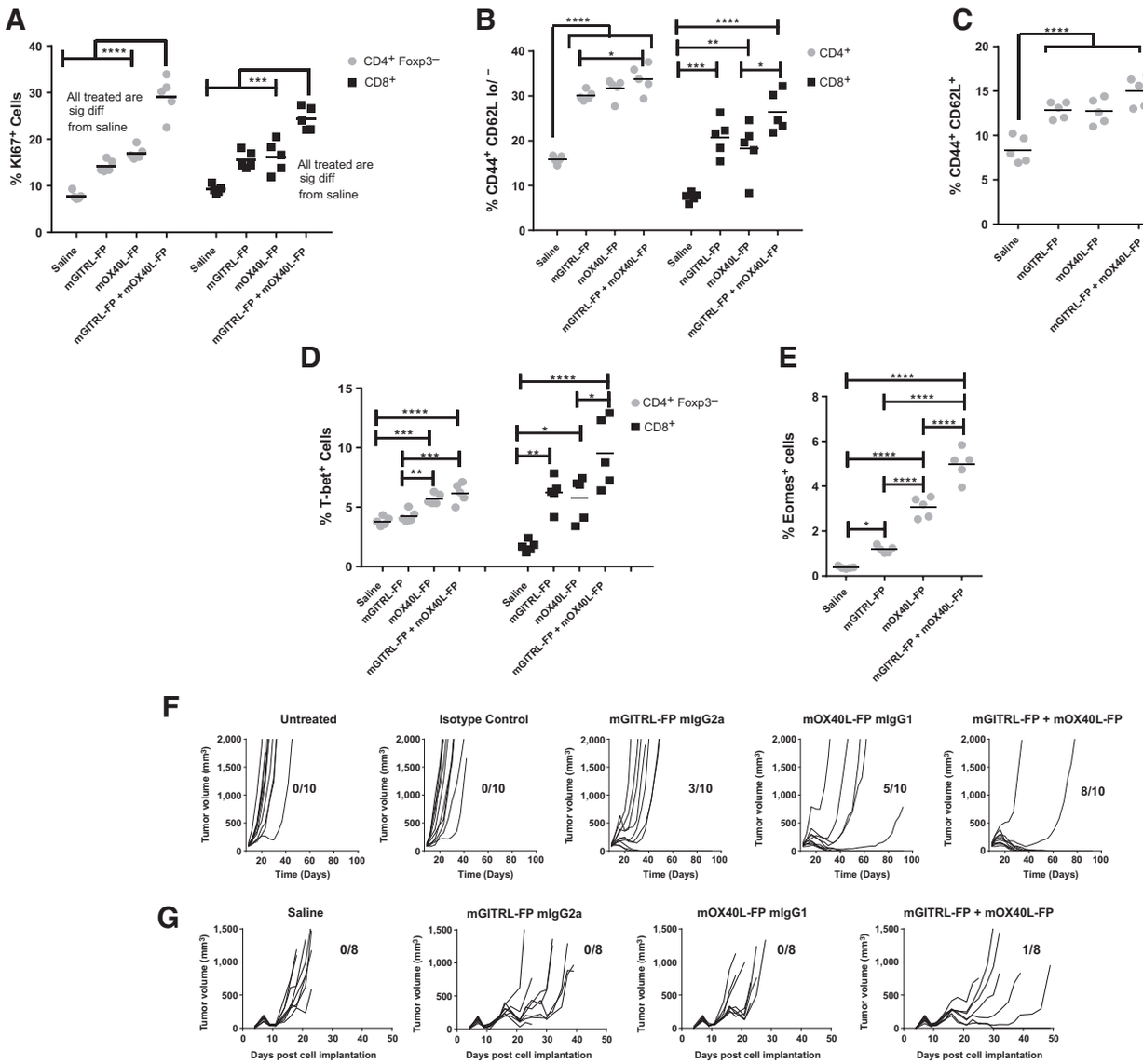

Figure 5.

Combination of mGITRL-FP mIgG2a and mOX40L-FP mIgG1 leads to enhanced T-cell activation and antitumor activity. Frequency of $CD4^+$ $FoxP3^-$ or $CD8^+$, $Ki67^+$ (**A**), $CD4^+$ or $CD8^+$, $CD44^+$ $CD62L^{lo/-}$ effector memory (**B**), $CD4^+$ $CD44^+$ $CD62L^+$ central memory (**C**), $CD4^+$ or $CD8^+$, T-bet^+ (**D**), and $CD4^+$ $Eomes^+$ T cells (**E**) in the spleens of CT26 tumor-bearing mice 14 days following twice weekly treatment with either 25 mg/kg mGITRL-FP mIgG2a, 15 mg/kg mOX40L-FP mIgG1, or a combination of both molecules. $N = 5$ mice per group. *, $P < 0.05$; **, $P < 0.01$; ***, $P < 0.001$; ****, $P < 0.0001$, as calculated by one-way ANOVA. **F,** CT26 tumor-bearing mice were untreated or treated by intraperitoneal injection of isotype control, 7.5 mg/kg of mOX40L-FP mIgG1 twice weekly for two doses, a single suboptimal dose of mGITRL-FP mIgG2a at 0.1 mg/kg or the combination of both molecules. **G,** B16F10-Luc2 tumor-bearing mice were dosed intraperitoneal with saline, 25 mg/kg mGITRL-FP mIgG2a biweekly for 2 weeks, 15 mg/kg mOX40L-FP mIgG1 bi-weekly for 3 weeks or a combination of both molecules and tumor growth measured. Number of total regressions are indicated next to each individual graph. Data are one representative of two independent experiments.

PD-L1 expression on splenic and intratumoral $CD8^+$ T cells and splenic $CD4^+$ T cells (Fig. 6A). There was no significant change in expression of PD-L1 on CT26 tumor cells, NK cells, or MDSCs ($Gr1^+$ $CD11b^+$ cells) after treatment with mGITRL-FP mIgG2a (data not shown). On the basis of this upregulation of PD-L1 expression, to define for the first time a proof of concept for the combination of a GITR agonist with a PD-L1 inhibitor, we combined a suboptimal dose of mGITRL-FP mIgG2a with anti-PD-L1 mIgG1 D265A. This molecule was engineered to target PD-L1 while limiting the binding to FcγRs, representing the closest mouse analogue for durvalumab (MEDI4736), an engineered hIgG1 anti-PD-L1 antibody currently in phase III clinical trials (24). The results showed a lack of complete tumor regression in the saline-treated control group, the NIP-228 mIgG1 D265A isotype control group, the anti-PD-L1 mIgG1 D265A-treated group, and the mGITRL-FP mIgG2a-treated group, despite the

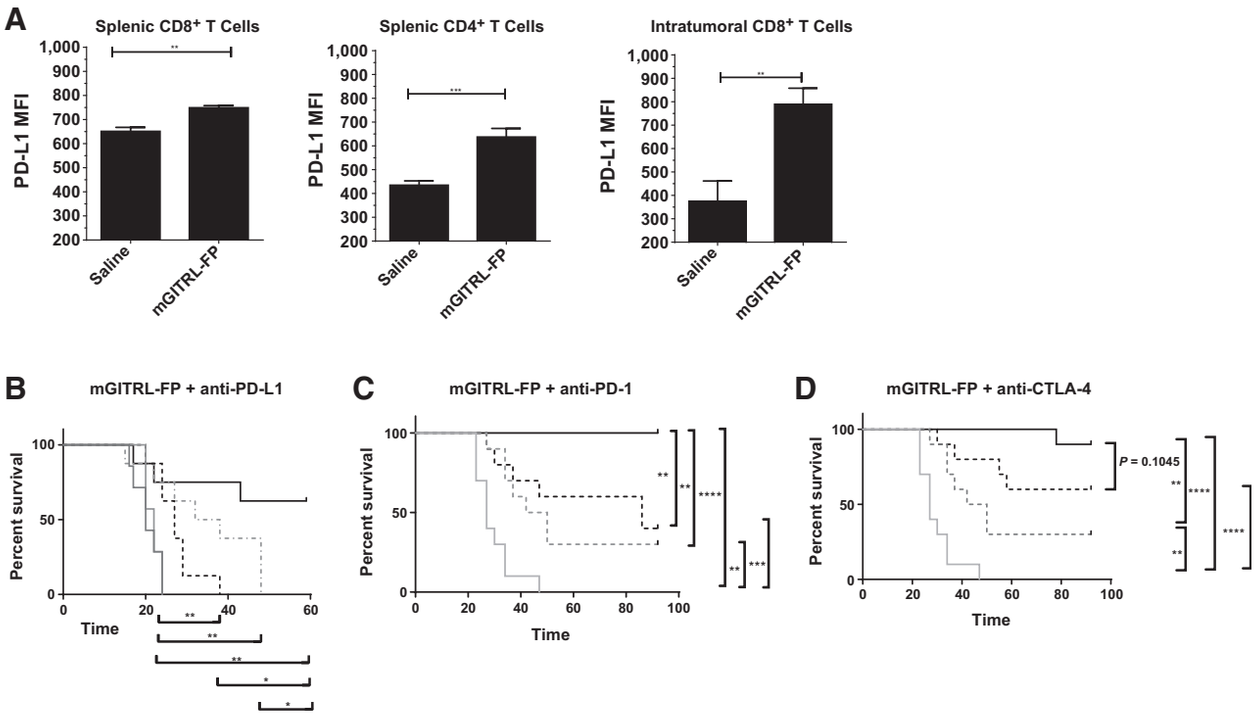

Figure 6.

The mGITRL-FP synergizes with checkpoint inhibitors to induce antitumor activity in CT26 tumor-bearing mice. **A,** PD-L1 MFI on splenic CD4$^+$ and CD8$^+$ T cells and intratumoral CD8$^+$ T cells, 7 days following treatment with a single intraperitoneal injection of saline control or 5 mg/kg mGITRL-FP mIgG2a. $N = 4$–5 mice per group, statistical significance calculated using unpaired Student *t* test, where **, $P < 0.01$ and ***, $P < 0.001$. Error bars, SEM. **B,** Kaplan–Meier survival curve of saline and isotype controls (solid light and dark gray lines), anti-PD-L1 mIgG1 D265A monotherapy (dotted black line), mGITRL-FP mIgG2a monotherapy (dotted gray line), or the combination of both molecules (solid black line). **C,** Survival of CT26 mice treated with saline (solid gray line), a single intraperitoneal injection of 0.1 mg/kg mGITRL-FP mIgG2a (dotted gray line), 20 mg/kg anti-PD-1 rIgG2a biweekly for two weeks (dotted black line) or a combination of both molecules (solid black line). **D,** Survival of CT26 mice treated with saline (solid gray line), a single intraperitoneal injection of 0.1 mg/kg mGITRL-FP mIgG2a (dotted gray line), 5 mg/kg anti-CTLA-4 mIgG2b twice weekly for 2 weeks (dotted black line), or a combination of both molecules (solid black line). Statistical significance for survival curves were carried out using log-rank (Mantel–Cox) test, where *, $P < 0.05$; **, $P < 0.01$; ***, $P < 0.001$; ****, $P < 0.0001$. Data are one representative of two independent experiments.

anti-PD-L1 monotherapy and mGITRL-FP mIgG2a monotherapy groups having significantly increased survival compared with control animals (Fig. 6B). However, the combination of both anti-PD-L1 mIgG1 D265A and mGITRL-FP mIgG2a resulted in a statistically significant increase in survival above all other treatment groups (Fig. 6B). We also observed an increase in the survival of mice treated with a combination of mGITRL-FP mIgG2a and anti-PD-1 rIgG2a or mGITRL-FP mIgG2a and anti-CTLA-4 mIgG2b compared with monotherapy treatment (Fig. 6C and D). Collectively, this preclinical data shows that mGITRL-FP mIgG2a can combine with antibodies targeting OX40 or checkpoint inhibitors.

Discussion

Targeting members of the TNFR superfamily, such as GITR and OX40, for cancer immunotherapy is emerging as a promising new approach (25–27). Both GITR and OX40 receptors are upregulated on CD4$^+$ and CD8$^+$ T cells following activation, and signaling via these receptors has been shown to drive the activation and antitumor activity of these cell types (27, 28). Although the rat IgG2b anti-murine GITR antibody DTA-1 has shown notable antitumor activity in several preclinical models (12, 29, 30), it is believed that higher order structures of GITRL can mediate stronger intracellular signals through their ability to drive greater aggregation of GITR as compared with an agonist antibody (17, 18), and as such a multivalent fusion protein could present an opportunity to deliver enhanced agonism of the GITR receptor.

Here we describe the characterization of a multimeric mGITRL-FP and its combination with a mOX40L-FP and investigate the simultaneous targeting of these two costimulatory receptor pathways in syngeneic tumor models. We demonstrate that this mGITRL-FP can efficiently bind to murine GITR, does not cross react with OX40 receptor and is able to elicit signaling in a NF-κB reporter cell assay with almost 50 times the potency of DTA-1. This enhanced agonistic potency *in vitro* was considered to be due to the increased valency of the multimeric mGITRL-FP, as compared with an anti-GITR antibody, which likely leads to enhanced crosslinking of GITR.

Previous studies (15) have indicated a requirement for FcγR binding for maximal activity of DTA-1. These studies compared a murine IgG2a isotype DTA-1 to one carrying the N297A mutation, which ablates FcγR binding, and showed that inclusion of this mutation totally abolished the antitumor activity of DTA-1. Here

we compared the activity of a mGITRL-FP of the mIgG2a isotype, which is considered to be one of the main effector function mediating isotypes *in vivo*, to that of a mIgG1 isotype, which is considered a low effector function mediating isotype. Mouse IgG2a is able to bind to FcγRI, FcγRIII, and FcγRIV, with the latter considered as the main activating receptor in mice due to IgG2a-dependent effector functions being severely impaired in the absence of this receptor *in vivo* (31). FcγRIV has been reported to be expressed on NK and myeloid cells in CT26 tumors (15) with the ability to mediate ADCC or ADCP (32). The mIgG1 isotype on the other hand is only able to bind to the inhibitory FcγRIIb and the low affinity activating FcγRIII (19), with no measurably affinity to FcγRIV. We show that, in contrast to previous findings with the N297A DTA-1, a mIgG1 mGITRL-FP can still mediate antitumor activity without the requirement to deplete intratumoral Tregs, although this activity is reduced as compared with the mIgG2a mGITRL-FP.

Both Fc variants of mGITRL-FPs efficiently enhanced proliferation of splenic effector T cells and Tregs *in vivo*, as measured by increases in the expression of Ki67. These data are consistent with the role of GITR as a costimulatory receptor on T cells, and which is similar to previous effects reported in GITRL transgenic mice (33) and in mice treated with Fc-GITRL dimers (34). The magnitude of the observed change in T-cell proliferation was not notably different when comparing the mIgG2a and mIgG1 mGITRL-FPs. This suggests that although the mIgG1 possesses reduced binding to FcγRs, as compared with the mIgG2a, that this does not impact its ability to be cross-linked sufficiently to mediate effective agonism of GITR. In contrast, modulation of intratumoral Tregs was found to be almost entirely dependent on Fc isotype, and was only observed following treatment with the mGITRL-FP mIgG2a. Concordant with this depletion of intratumoral Tregs was an increase in the CD8:Treg and CD4:Treg ratio, leading to an increase in antitumor activity. Moreover, due to the lack of Treg depletion with the mIgG1 isotype, these data build on previous findings (15) with respect to the role of Fc isotype in the activity of GITR-targeting agents, by suggesting that Treg depletion is not a requisite for antitumor activity, but rather functions to enhance the activity already observed through agonism of GITR.

Further characterization of the mGITRL-FP mIgG2a showed that the antitumor activity in CT26 tumor-bearing mice was dose dependent, and could be correlated with the expression of pharmacodynamic biomarkers of proliferation (Ki67) and activation (ICOS and PD-l) in peripheral T cells. These dose–response studies indicated that sustained exposure of the mGITRL-FP was required to induce optimal antitumor activity. Pharmacokinetic modeling and simulation, based on a single-dose pharmacokinetic study, suggested that a threshold concentration of 1 μg/mL was associated with this optimal antitumor activity. Such data could be used to assist planning of the clinical testing of similar molecules in humans, as has been reported for other cancer therapies (35, 36).

Another member of the TNFR superfamily which shares high functional homology to GITR is OX40. The binding of OX40L to OX40, which has been reported to be preferentially expressed on CD4 T cells as opposed to CD8 T cells, induces activation, survival, and proliferation (37–40) and in addition has been shown to deactivate the immunosuppressive capacity of Tregs (41). Similarly to targeting of GITR, OX40 agonism-mediated antitumor immunity in murine tumor models has also been shown to require binding of activatory FcγRs to induce intratumoral Treg depletion (20). To attempt to evaluate differences in GITR and OX40 agonism-mediated antitumor activity, we directly compared the tumor growth of CT26 tumor-bearing mice which had been treated with either a mOX40L-FP or a mGITRL-FP composed of mIgG1 or mIgG2a isotypes. As expected, all four FPs mediated some antitumor activity; for both mOX40L-FP and mGITRL-FP antitumor activity was more robust when using a FP of the mIgG2a isotype, and in both cases this increased antitumor activity was coincident with intratumoral Treg reduction that was not observed with the mIgG1 isotype. Pharmacodynamic analyses following treatment of tumor-bearing mice with mGITRL-FP or mOX40L-FP at high doses showed that the mOX40L-FP mIgG1 monotherapy treatment induced a significantly higher frequency of $CD4^+$ T cells expressing the Th1 transcription factors T-bet and Eomes in $CD4^+$ T cells than did mGITRL-FP mIgG2a monotherapy, indicating a more prominent role for OX40 in $CD4^+$ Th1 differentiation than GITR. The combination of both mGITRL-FP mIgG2a and mOX40L-FP mIgG1 was able to enhance the proportion of central memory and effector memory T-cell populations, the expression of transcription factors T-bet and Eomes and the proliferation of T cells, as measured by Ki67 expression, above that observed with either FP as monotherapy. These data suggested there may be a nonredundant role for the GITR and OX40 pathways with respect to T-cell activation, and prompted the testing of the combination of mGITRL-FP and mOX40L-FP with respect to antitumor activity.

To assess combination activity of mGITRL-FP and mOX40L-FP, two alternative studies were conducted using mGITRL-FP mIgG2a and mOX40L-FP mIgG1, which were selected on the basis of their ability to most closely mimic the FcγR-binding properties of the clinical candidates MEDI6363 and MEDI1873. The first study was conducted in CT26 where, given the curative nature of mGITRL-FP mIgG2a, a maximally active dose of mOX40L-FP mIgG1 was combined with a single suboptimal dose of mGITRL-FP mIgG2a and was able to show improved antitumor activity compared with monotherapy treatment. The second study was conducted in B16F10-Luc2, which is an example of an immunologically "cold" tumor with significantly reduced immune cell infiltration when compared with the CT26 model (42). In this model, monotherapy activity for either molecule was minimal; however, the combination of the two FPs at high doses resulted in a notable increase in antitumor activity.

The mGITRL-FP mIgG2a has been previously reported to synergize with chemotherapeutic agents (43). In this report, we build on this data by showing enhanced activity in combination with a mOX40L-FP, with this data being the first to show a beneficial effect from targeting the OX40 and GITR pathways in combination for cancer immunotherapy. Furthermore, we show that the mGITRL-FP can effectively combine with anti-PD-1 or anti-CTLA-4, as has been shown for other GITR agonists (44, 45) and demonstrate for the first time that a GITR agonist can synergize with anti-PD-L1.

Antibodies targeting PD-L1, PD-1, and CTLA-4 receptors have already been approved in a number of indications and there is tremendous potential for the combination of these immuno-oncology agents for cancer therapy (46). Several GITR-targeting agents, including a number of mAbs (47), as well as GITRL-

expressing dendritic cells (DC) are already in clinical trials, as are a number of OX40 agonists (22), including the human OX40L-FP MEDI6383 and humanized anti-human OX40 mAb MEDI0562. This preclinical data provides evidence that targeting of GITR represents a unique approach to cancer immunotherapy, distinct and nonredundant to OX40 targeting, and suggests that a multimeric FP may provide increased agonistic potential versus an antibody. In addition these data provide, for the first time, early proof of concept for the potential combination of GITR agonists with OX40- or PD-L1–targeting agents. On the basis of these, and additional studies, the human IgG1 GITRL-FP, MEDI1873, is currently in phase I clinical trials in patients with advanced solid tumors.

Disclosure of Potential Conflicts of Interest

M.D. Oberst and R. Stewart hold ownership interest (including patents) in AstraZeneca. No potential conflicts of interest were disclosed by the other authors.

Authors' Contributions

Conception and design: R. Leyland, A. Watkins, L. Young, S.A. Hammond, R. Stewart

Development of methodology: R. Leyland, A. Watkins, K.A. Mulgrew, L. Yan, M.D. Oberst, C.C. Leow, R. Stewart

Acquisition of data (provided animals, acquired and managed patients, provided facilities, etc.): R. Leyland, N.J. Tigue, E. Offer, J. Andrews, S. Mullins, J. Coates Ulrichsen, D.A. Leinster, K. McGlinchey, L. Young

Analysis and interpretation of data (e.g., statistical analysis, biostatistics, computational analysis): R. Leyland, A. Watkins, K.A. Mulgrew, N. Holoweckyj, E. Offer, J. Andrews, L. Yan, S. Mullins, M.D. Oberst, M. Morrow, S.A. Hammond, P. Mallinder, A. Herath, C.C. Leow, R.W. Wilkinson, R. Stewart

Writing, review, and/or revision of the manuscript: R. Leyland, A. Watkins, K.A. Mulgrew, N. Holoweckyj, N.J. Tigue, M.D. Oberst, K. McGlinchey, L. Young, M. Morrow, S.A. Hammond, P. Mallinder, A. Herath, C.C. Leow, R.W. Wilkinson, R. Stewart

Administrative, technical, or material support (i.e., reporting or organizing data, constructing databases): R. Leyland, A. Watkins, L. Bamber, M. Morrow

Study supervision: R. Leyland, M. Morrow, C.C. Leow

Acknowledgments

The authors thank the Biological Services team for their support in conducting murine studies, the tissue culture team for providing syngeneic cell lines, Janette Dillon for generating the B16F10-Luc2 syngeneic cell line, and Claire Dobson, Jenny Percival-Alwyn, Jayne Hammersley, Ling Huang, and Maria Groves for generation of the anti-PD-L1 mIgG1 D265A molecule.

Grant Support

All studies were funded by MedImmune.

The costs of publication of this article were defrayed in part by the payment of page charges. This article must therefore be hereby marked *advertisement* in accordance with 18 U.S.C. Section 1734 solely to indicate this fact.

Received August 16, 2016; revised December 14, 2016; accepted January 2, 2017; published OnlineFirst January 9, 2017.

References

1. Zou W. Regulatory T cells, tumour immunity and immunotherapy. Nat Rev Immunol 2006;6:295–307.
2. Ronchetti S, Zollo O, Bruscoli S, Agostini M, Bianchini R, Nocentini G, et al. GITR, a member of the TNF receptor superfamily, is costimulatory to mouse T lymphocyte subpopulations. Eur J Immunol 2004;34:613–22.
3. Tone M, Tone Y, Adams E, Yates SF, Frewin MR, Cobbold SP, et al. Mouse glucocorticoid-induced tumor necrosis factor receptor ligand is costimulatory for T cells. Proc Natl Acad Sci U S A 2003;100:15059–64.
4. Ramirez-Montagut T, Chow A, Hirschhorn-Cymerman D, Terwey TH, Kochman AA, Lu S, et al. Glucocorticoid-induced TNF receptor family related gene activation overcomes tolerance/ignorance to melanoma differentiation antigens and enhances antitumor immunity. J Immunol 2006; 176:6434–42.
5. Stephens GL, McHugh RS, Whitters MJ, Young DA, Luxenberg D, Carreno BM, et al. Engagement of glucocorticoid-induced TNFR family-related receptor on effector T cells by its ligand mediates resistance to suppression by CD4+CD25+ T cells. J Immunol 2004;173:5008–20.
6. Nishikawa H, Kato T, Hirayama M, Orito Y, Sato E, Harada N, et al. Regulatory T cell-resistant CD8+ T cells induced by glucocorticoid-induced tumor necrosis factor receptor signaling. Cancer Res 2008;68:5948–54.
7. Ji HB, Liao G, Faubion WA, Abadia-Molina AC, Cozzo C, Laroux FS, et al. Cutting edge: the natural ligand for glucocorticoid-induced TNF receptor-related protein abrogates regulatory T cell suppression. J Immunol 2004; 172:5823–7.
8. Schaer DA, Budhu S, Liu C, Bryson C, Malandro N, Cohen A, et al. GITR pathway activation abrogates tumor immune suppression through loss of regulatory T cell lineage stability. Cancer Immunol Res 2013;1:320–31.
9. McHugh RS, Shevach EM. The role of suppressor T cells in regulation of immune responses. J Allergy Clin Immunol 2002;110:693–702.
10. Shimizu J, Yamazaki S, Takahashi T, Ishida Y, Sakaguchi S. Stimulation of CD25(+)CD4(+) regulatory T cells through GITR breaks immunological self-tolerance. Nat Immunol 2002;3:135–42.
11. Ko K, Yamazaki S, Nakamura K, Nishioka T, Hirota K, Yamaguchi T, et al. Treatment of advanced tumors with agonistic anti-GITR mAb and its effects on tumor-infiltrating Foxp3+CD25+CD4+ regulatory T cells. J Exp Med 2005;202:885–91.
12. Zhou P, L'Italien L, Hodges D, Schebye XM. Pivotal roles of CD4+ effector T cells in mediating agonistic anti-GITR mAb-induced-immune activation and tumor immunity in CT26 tumors. J Immunol 2007;179: 7365–75.
13. Liu Z, Tian S, Falo LDJr, Sakaguchi S, You Z. Therapeutic immunity by adoptive tumor-primed CD4(+) T-cell transfer in combination with in vivo GITR ligation. Mol Ther 2009;17:1274–81.
14. Cohen AD, Schaer DA, Liu C, Li Y, Hirschhorn-Cymmerman D, Kim SC, et al. Agonist anti-GITR monoclonal antibody induces melanoma tumor immunity in mice by altering regulatory T cell stability and intra-tumor accumulation. PLoS One 2010;5:e10436.
15. Bulliard Y, Jolicoeur R, Windman M, Rue SM, Ettenberg S, Knee DA, et al. Activating Fc gamma receptors contribute to the antitumor activities of immunoregulatory receptor-targeting antibodies. J Exp Med 2013;210: 1685–93.
16. Clouthier DL, Watts TH. Cell-specific and context-dependent effects of GITR in cancer, autoimmunity, and infection. Cytokine Growth Factor Rev 2014;25:91–106.
17. Zhou Z, Song X, Berezov A, Zhang G, Li Y, Zhang H, et al. Human glucocorticoid-induced TNF receptor ligand regulates its signaling activity through multiple oligomerization states. Proc Natl Acad Sci U S A 2008; 105:5465–70.
18. Zhou Z, Tone Y, Song X, Furuuchi K, Lear JD, Waldmann H, et al. Structural basis for ligand-mediated mouse GITR activation. Proc Natl Acad Sci U S A 2008;105:641–5.
19. Stewart R, Hammond SA, Oberst M, Wilkinson RW. The role of Fc gamma receptors in the activity of immunomodulatory antibodies for cancer. J Immunother Cancer 2014;2:29.
20. Bulliard Y, Jolicoeur R, Zhang J, Dranoff G, Wilson NS, Brogdon JL. OX40 engagement depletes intratumoral Tregs via activating FcgammaRs, leading to antitumor efficacy. Immunol Cell Biol 2014;92:475–80.
21. Clynes RA, Towers TL, Presta LG, Ravetch JV. Inhibitory Fc receptors modulate in vivo cytotoxicity against tumor targets. Nat Med 2000; 6:443–6.
22. Aspeslagh S, Postel-Vinay S, Rusakiewicz S, Soria JC, Zitvogel L, Marabelle A. Rationale for anti-OX40 cancer immunotherapy. Eur J Cancer 2016; 52:50–66.

23. Pearce EL, Mullen AC, Martins GA, Krawczyk CM, Hutchins AS, Zediak VP, et al. Control of effector CD8+ T cell function by the transcription factor Eomesodermin. Science 2003;302:1041–3.
24. Stewart R, Morrow M, Hammond SA, Mulgrew K, Marcus D, Poon E, et al. Identification and characterization of MEDI4736, an antagonistic anti-PD-L1 monoclonal antibody. Cancer Immunol Res 2015;3:1052–62.
25. Croft M, Benedict CA, Ware CF. Clinical targeting of the TNF and TNFR superfamilies. Nat Rev Drug Discov 2013;12:147–68.
26. Sugamura K, Ishii N, Weinberg AD. Therapeutic targeting of the effector T-cell co-stimulatory molecule OX40. Nat Rev Immunol 2004;4:420–31.
27. Schaer DA, Murphy JT, Wolchok JD. Modulation of GITR for cancer immunotherapy. Curr Opin Immunol 2012;24:217–24.
28. Redmond WL, Weinberg AD. Targeting OX40 and OX40L for the treatment of autoimmunity and cancer. Crit Rev Immunol 2007;27:415–36.
29. Cohen AD, Diab A, Perales MA, Wolchok JD, Rizzuto G, Merghoub T, et al. Agonist anti-GITR antibody enhances vaccine-induced CD8(+) T-cell responses and tumor immunity. Cancer Res 2006;66:4904–12.
30. Coe D, Begom S, Addey C, White M, Dyson J, Chai JG. Depletion of regulatory T cells by anti-GITR mAb as a novel mechanism for cancer immunotherapy. Cancer Immunol Immunother 2010;59:1367–77.
31. Nimmerjahn F, Lux A, Albert H, Woigk M, Lehmann C, Dudziak D, et al. FcgammaRIV deletion reveals its central role for IgG2a and IgG2b activity in vivo. Proc Natl Acad Sci U S A 2010;107:19396–401.
32. Nimmerjahn F, Ravetch JV. Fcgamma receptors as regulators of immune responses. Nat Rev Immunol 2008;8:34–47.
33. van Olffen RW, Koning N, van Gisbergen KP, Wensveen FM, Hoek RM, Boon L, et al. GITR triggering induces expansion of both effector and regulatory CD4+ T cells in vivo. J Immunol 2009;182:7490–500.
34. Kim YH, Shin SM, Choi BK, Oh HS, Kim CH, Lee SJ, et al. Authentic GITR signaling fails to induce tumor regression unless Foxp3+ regulatory T cells are depleted. J Immunol 2015;195:4721–9.
35. Tanaka C, O'Reilly T, Kovarik JM, Shand N, Hazell K, Judson I, et al. Identifying optimal biologic doses of everolimus (RAD001) in patients with cancer based on the modeling of preclinical and clinical pharmacokinetic and pharmacodynamic data. J Clin Oncol 2008;26:1596–602.
36. Derendorf H, Meibohm B. Modeling of pharmacokinetic/pharmacodynamic (PK/PD) relationships: concepts and perspectives. Pharm Res 1999;16:176–85.
37. Weinberg AD, Rivera MM, Prell R, Morris A, Ramstad T, Vetto JT, et al. Engagement of the OX-40 receptor in vivo enhances antitumor immunity. J Immunol 2000;164:2160–9.
38. Rogers PR, Song J, Gramaglia I, Killeen N, Croft M. OX40 promotes Bcl-xL and Bcl-2 expression and is essential for long-term survival of CD4 T cells. Immunity 2001;15:445–55.
39. Redmond WL, Ruby CE, Weinberg AD. The role of OX40-mediated co-stimulation in T-cell activation and survival. Crit Rev Immunol 2009;29:187–201.
40. Gramaglia I, Jember A, Pippig SD, Weinberg AD, Killeen N, Croft M. The OX40 costimulatory receptor determines the development of CD4 memory by regulating primary clonal expansion. J Immunol 2000;165:3043–50.
41. Schaer DA, Hirschhorn-Cymerman D, Wolchok JD. Targeting tumor-necrosis factor receptor pathways for tumor immunotherapy. J Immunother Cancer 2014;2:7.
42. Mosely SI, Prime JE, Sainson RC, Koopmann JO, Wang DY, Greenawalt DM, et al. Rational selection of syngeneic preclinical tumor models for immunotherapeutic drug discovery. Cancer Immunol Res 2017;5:29–41.
43. Rios-Doria J, Durham N, Wetzel L, Rothstein R, Chesebrough J, Holoweckyj N, et al. Doxil synergizes with cancer immunotherapies to enhance anti-tumor responses in syngeneic mouse models. Neoplasia 2015;17:661–70.
44. Mitsui J, Nishikawa H, Muraoka D, Wang L, Noguchi T, Sato E, et al. Two distinct mechanisms of augmented antitumor activity by modulation of immunostimulatory/inhibitory signals. Clin Cancer Res 2010;16:2781–91.
45. Lu L, Xu X, Zhang B, Zhang R, Ji H, Wang X. Combined PD-1 blockade and GITR triggering induce a potent antitumor immunity in murine cancer models and synergizes with chemotherapeutic drugs. J Transl Med 2014;12:36.
46. Melero I, Berman DM, Aznar MA, Korman AJ, Perez Gracia JL, Haanen J. Evolving synergistic combinations of targeted immunotherapies to combat cancer. Nat Rev Cancer 2015;15:457–72.
47. Knee DA, Hewes B, Brogdon JL. Rationale for anti-GITR cancer immunotherapy. Eur J Cancer 2016;67:1–10.